Propagation and direction finding of Schumann resonances in relation with the global thunderstorm activity

Tsuyoshi Hayashida[1], Yasuhide Hobara[2], Natsuko Iwasaki[1] and Masashi Hayakawa[1]

[1] The University of Electro-Communications, Chofu Tokyo

[2] Earth Observation Research Center, NASDA

[1] 1-5-1 Chofugaoka, Chofu-shi, Tokyo, 182-8585 JAPAN

[2] 1-9-9 Roppongi Minato-ku Tokyo, 106-0032 Japan

E-mail hayasida@whistler.ee.uec.ac.jp

1. Introduction

A lightning discharge radiates a broadband electromagnetic impulse that spreads laterally away from the source into the earth-ionosphere cavity. The lowest frequency components of the impulse can circumnavigate the globe several times before suffering considerable attenuation and create a resonance phenomenon inside the earth-ionosphere cavity; so called Schumann resonances (SR). They have line spectral components at approximately 8,14,20 Hz and higher frequencies. SR magnitude in electric and magnetic fields show diurnal and seasonal variations mainly due to the global thunderstorm activity change, however the identification and quantitative information of the source of SR have not been derived well. Besides, SR are not a purely resonant phenomenon and have propagating modes because of the poor conductivity and day-night asymmetry of the height in the ionospheric height.

In this study, we perform the direction finding of these traveling waves in SR components observed at Moshiri to determine the source bearing (azimuth) using the Poynting vector for April 8 1999. Next, we derive the source-observer distance by using the wave impedance method by using electric and magnetic field components. As a result, we successfully obtained the arrival direction and reasonable distance from the three main thunderstorm active regions. Further we compare our results from SR with the satellite data observing the optical emission from the lightning.

2. Observation System

We started the wide-band ELF measurement at Moshiri observatory (44° 21' 9"N, 142° 15' 61"E) in Hokkaido in November, 1996 with the vertical electric field component ($Ez(f)$) by a capacitor type antenna and two horizontal magnetic field components (East-West component ($Hew(f)$) and North-South component ($Hns(f)$)) with sampling frequency of 2kHz. We separate the system into two parts; one for SR and another for ELF transients. For SR measurement, we record the complex Fourier components averaged every 10 minutes for the frequency up to 1kHz with 2Hz resolution for all three field components. Besides all the components are absolutely calibrated, which enable us to deduce the quantitative information about the source.

3. Experimental Results

Global thunderstorm activity is concentrated over the continents in the tropical zone. There are three main global thunderstorm centers over Africa, America, and South-East

Asia. Activity at each thunderstorm center reaches its maximum just after the local afternoon, which corresponds to the time around 8 hr in Asia, 14 hr in Africa and 21 hr UT in America respectively when we observe the largest magnitude during a day.

3.1. Diurnal variation of Schumann resonance

We measure the magnitude and phase of frequency components within ±0.5Hz just around the first three resonance frequencies, and averaged every 10 minutes. We show the diurnal pattern of Hew and Hns for the second mode (14Hz) of SR in Figures 2 (a) and 2 (b).

3.2. Diurnal variation of direction finding of the global thunderstorm activity

SR are poor resonance phenomena in the sense that most of them have traveling components. So we can perform the direction finding using Poynting vector method. The coordinate system used for direction finding is illustrated in Figure 1.
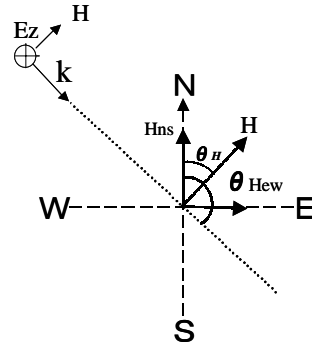

Figure 1: Coordinate system for direction finding.

First of all we derive direction (θ_H) of the total magnetic components of the wave with an ambiguity of 180º from eq. (1).

$$\theta_H = \tan^{-1}\left(\frac{Ez(f) \cdot Hns(f)}{-Ez(f) \cdot Hew(f)} \right) \tag{1}$$

where Ez(f) is the magnitude of vertical electric field component in frequency domain and Hns(f) and Hew(f) are the magnitudes of two horizontal magnetic field components in the frequency domain.

And then we can specify the particular quadrant using the phase difference between Ez and Hns and obtain the wave normal direction of the wave by adding 90º to θ_H. Figure 2 (c) shows the diurnal pattern of the arrival direction calculated for the second mode of SR.

3.3. Distance estimation of thunderstorm centers

First of all we calculate the frequency variation of the wave impedance by eq. (2).

$$z(f) = \frac{Ez(f)}{\sqrt{Hew(f)^2 + Hns(f)^2}} \cos\phi(f) \tag{2}$$

where ϕ(f) is the phase difference between Ez and Hns. To reduce the effect of the

fluctuation in frequency and time, we use each frequency component in eq. (2) by taking the running mean over ± 2Hz, and the time evolution of $z(f)$ is obtained by the produce of running average over ± 10 minutes. At each moment we compute the source-observer distance by using cross-correlation analysis between the experimental $z(f)$ and theoretical one, which is shown in Figure 2 (d).
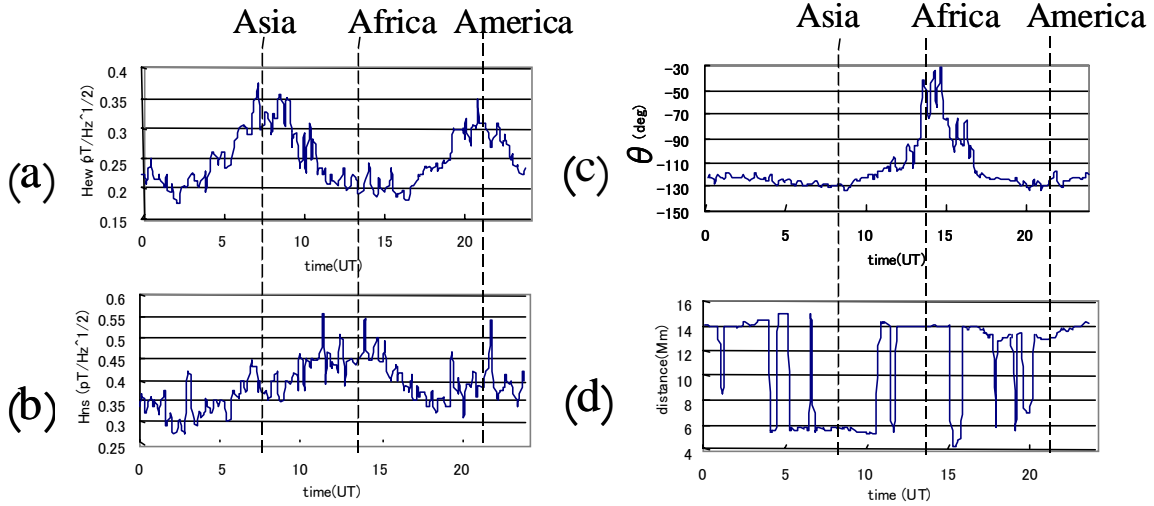

Figure 2: (a) Diurnal pattern of Hew for the second mode of SR. (b) Diurnal pattern of Hns for the second mode of SR. (c) Diurnal pattern of arrival direction for the second mode of SR. (d) Diurnal pattern of calculated source-receiver distance.

4. Discussion

We pay attention to the point of intersection between dotted lines and the variation in each graph in Figures 2(a)-2(d). Dotted lines represent the time of thunderstorm activity peak during day at each of three thunderstorm centers.

Figures 2 (a) and 2 (b) show the diurnal pattern of SR magnitude for Hew, Hns respectively for the second resonance frequency component. As is seen in Figures 2 (a) and (b), the peak times of the diurnal pattern coincide with the local afternoons of the three major thunderstorm regions. It implies that most lightning discharges from these three regions play a significant role in the diurnal pattern of SR magnitude.

Figures 2 (c) and 2 (d) show the results of direction finding and distance estimation respectively. Three dotted lines in Figure 2 coincide with the local maxima of the thunderstorm activity in Asia, Africa and America. As is seen in Figure 2 (c), we obtain the arrival direction for Asian source as -130 deg. For Africa and American source, we one get −46 deg and -125 deg respectively. According to Figure 2 (d), calculated distance to the Asian source is 5.5 Mm and 14 Mm and 13 Mm for Africa and America, respectively.

Further Figure 3 illustrates the azimuthal equidistant projection around Hokkaido in the global map with calculated arrival angle shown by lines, and distances shown in circles for three thunderstorm regions.

Now we can consider the validity of our estimation on the source location of each thunderstorm center from Figure 3. First of all the intersection between estimated

distance and arrival direction of American source is located in the central part in the Pacific and a coastal region of the Gulf of Mexico. While we obtain the active thunderstorm regions for Asian and African source at the northern west-coast of America and at the center of the Pacific Ocean where lightning activity is infrequent. Probably, the phase estimation between Ez and Hns components did not work well in this case. We should improve the situation by changing the time period used for FFT analysis.

If we assume the 180º ambiguity for these results, we get active regions for Asian source in Indonesian region and for African source in the Congo basin where a lot of lightning occur discharges for another possible quadrant. In the case of American source, location of another quadrant is on the sea where lightning activity is not strong in general, hence our estimation of direction finding for this region is correct.

Finally we compare our results based on SR observation with the data of one-month averaged Optical Transient Detector (OTD) aboard the satellite by NASA for April 1998 shown in Figure 4. As is seen from Figure 4 lightning discharge occurs frequently around Indonesia, Congo basin and the coastal place of the Gulf of Mexico.
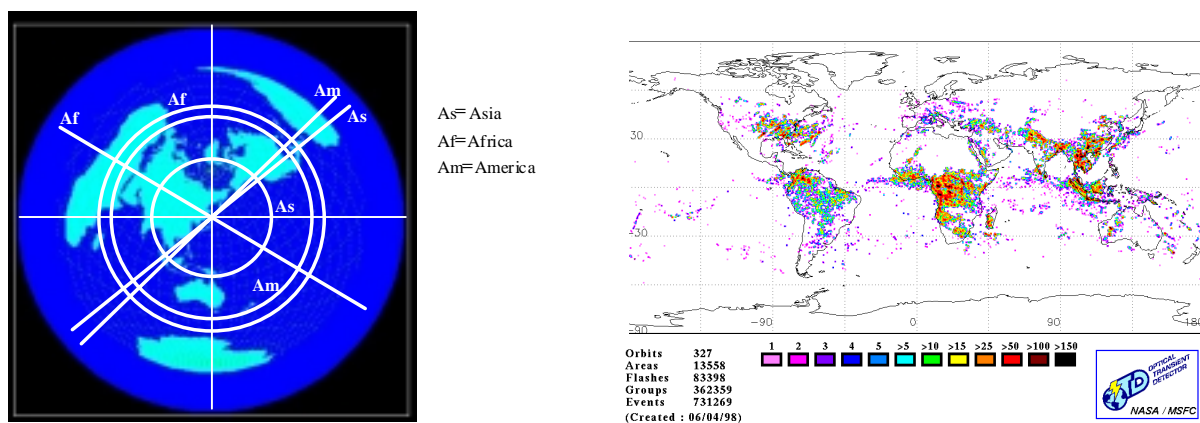

Figure 3: (left) The azimuthal equidistant projection around Hokkaido in the global map with calculated arrival angle shown by lines, and distances shown in circles for three thunderstorm regions

Figure 4: (right) Observation data of one-month averaged Optical Transient Detector (OTD) on band the satellite by NASA for April 1998

In summary, we have a good agreement between the location of main three thunderstorm regions derived by our SR measurement and the results from direct observation by satellite.

Further averaged quantitative information of the lightning activity like charge moment can be derived.

5.References

Sentman, D.D., Schumann Resonances, Handbook of Atmospheric Elecrodynamics, vol. 1 Pages 267-295, CRC Press, 1995.

Galejs, J., E.L.F. Propagation and Schumann Resonances, Terrestrial propagation of long electromagnetic waves, Pages 239-298, 1972.